

# Elasticity and piezoelectricity of zinc oxide crystals, single layers, and possible single-walled nanotubes

Z. C. Tu and X. Hu

*Computational Materials Science Center,*

*National Institute for Materials Science, Tsukuba 305-0047, Japan*

## Abstract

The elasticity and piezoelectricity of zinc oxide (ZnO) crystals and single layers are investigated from the first-principles calculations. It is found that a ZnO thin film less than three Zn-O layers prefers a planar graphite-like structure to the wurtzite structure. ZnO single layers are much more flexible than graphite single layers in the elasticity and stronger than boron nitride single layers in the piezoelectricity. Single-walled ZnO nanotubes (SWZONTs) can exist in principle because of their negative binding energy. The piezoelectricity of SWZONTs depends on their chirality. For most ZnO nanotubes except the zigzag type, twists around the tube axis will induce axial polarizations. A possible scheme is proposed to achieve the SWZONTs from the solid-vapor phase process with carbon nanotubes as templates.

PACS numbers: 62.25.+g, 62.20.Dc, 77.65.-j

## I. INTRODUCTION

Zinc oxide (ZnO) materials have attracted extensive attention for half a century because of their excellent performance in optics, electronics and photoelectronics.<sup>1</sup> They are important for low cost productions of green, blue-ultraviolet, and white light-emitting devices due to their wide band gap ( $\sim 3.37$  eV) and large exciton binding energy ( $\sim 60$  meV). They can also be used as sensors and transducers owing to their strong piezoelectricity. Recently, many ZnO nanostructures have been synthesized in experiments.<sup>2</sup> Among them, the quasi-one-dimensional structures have become the leading research objects because of their novel chemical, electrical, mechanical and optical properties.<sup>3</sup> The ultraviolet lasing in ZnO nanowires<sup>4,5</sup> and strong photoluminescence in ZnO nanorods<sup>6</sup> have been demonstrated. Nanobelts, nanorings and nanohelices are also synthesized,<sup>7,8,9,10</sup> which may be useful for field-effect transistors.<sup>11</sup>

Since the discovery of carbon nanotubes in 1991,<sup>12</sup> the synthesis of tubular nanostructures has raised worldwide interest. A lot of inorganic nanotubes, such as ZrS<sub>2</sub>, NbSe<sub>2</sub>, SiO<sub>2</sub>, TiO<sub>2</sub>, BN nanotubes, etc. are achieved by several groups.<sup>13</sup> Researchers have also tried to fabricate ZnO nanotubes through various methods including thermal reduction,<sup>14</sup> vapor phase growth,<sup>15,16,17</sup> hydrothermal growth,<sup>18</sup> vapor-solid process,<sup>19</sup> sol-gel template process,<sup>20</sup> plasma-assisted molecular beam epitaxy,<sup>21,22</sup> pyrolysis of zinc acetylacetonate,<sup>23</sup> and Zn(NH<sub>3</sub>)<sub>4</sub><sup>2+</sup> precursor thermal decomposition.<sup>24</sup> All ZnO nanotubes thus obtained have the wurtzite structure with diameter of 30–450 nm and thickness of 4–100 nm. Much effort has been made to realize much thinner and smaller ZnO nanotubes. A natural question is: Can we manufacture single-walled ZnO nanotubes (SWZONTs)? In this paper, We will answer this question based on the first-principles calculations (the ABINIT package<sup>25</sup>) and the experimental methods<sup>15,16,17,19</sup> for synthesizing ZnO nanobelts and nanotubes with the wurtzite structure. Additionally, we will investigate the elasticity and piezoelectricity of ZnO crystals and single layers within the framework of density-functional theory (DFT)<sup>26</sup> and density-functional perturbation theory (DFPT).<sup>27,28,29</sup> The piezoelectricity of single-walled ZnO nanotubes is also derived from the piezoelectricity of ZnO single layers.

The rest of this paper is organized as follows: In Sec. II, we present the results of elastic constants and piezoelectric coefficients of ZnO crystals. We also compare them with the experimental results and previous theoretical results in literatures. The main aim of this

section is to test whether our computational procedure can validly describe the physical properties of the ZnO system or not. In Sec. III, we optimize a Zn-O single layer cut from the wurtzite crystal and arrive at a planar graphite-like structure. Comparing the binding energy between the crystal and the planar single layer, we deduce that a ZnO thin film less than three Zn-O layers prefers a planar graphite-like structure to the wurtzite structure. The elastic and piezoelectric constants of ZnO single layers are also calculated. In Sec. IV, we calculate and optimize different SWZONTs. The SWZONTs are shown to exist in principle because of their negative binding energy. Their piezoelectricity depends on the chirality, and for most of them except the zigzag type, twists around the tube axis will induce axial polarizations. We also propose a possible scheme to realize the SWZONTs from the solid-vapor phase process with carbon nanotubes as templates. In Sec. V, we give a summary and propose some potential applications of SWZONTs.

## II. ZINC OXIDE CRYSTALS

The ground state of a ZnO crystal has a wurtzite structure (space group  $P6_3mc$ ) with two zinc and two oxygen atoms per unit cell. The lattice constants and internal parameter obtained from experiments are as follows:  $a = b = 3.250\text{\AA}$ ,  $c = 5.204\text{\AA}$ , and  $u = 0.382$ , respectively.<sup>30</sup>

We optimize the structure parameters and calculate the elastic and piezoelectric constants of ZnO crystals. The calculations are carried by taking Troullier-Martins pseudopotentials,<sup>31</sup> plane-wave energy cutoff (ecut) of 60 Hartree, and  $6 \times 6 \times 3$  Monkhorst-Pack k-points<sup>32</sup> in Brillouin-zone. The exchange-correlation energy are treated within the local-density approximation in the Ceperley-Alder form<sup>33</sup> with the Perdew-Wang parametrization.<sup>34</sup>

Using the experimental parameters to construct an initial unit cell, we have optimized the structure parameters and summarized them in Table I. Results by other groups are also listed for comparison. It is easy to see that our DFT results are quite close to those of Wu *et al.* and agree well with the experimental results (errors in 2%).

Adopting the optimized structure, we can calculate the elastic constants and piezoelectric coefficients of ZnO crystals. The elastic constants reflect the stress-strain relation of materials. In terms of the symmetry of ZnO crystals (wurtzite structure), this relation can

be expressed in the matrix form:<sup>37</sup>

$$\begin{bmatrix} \sigma_1 \\ \sigma_2 \\ \sigma_3 \\ \sigma_4 \\ \sigma_5 \\ \sigma_6 \end{bmatrix} = \begin{bmatrix} c_{11} & c_{12} & c_{13} & 0 & 0 & 0 \\ c_{12} & c_{11} & c_{13} & 0 & 0 & 0 \\ c_{13} & c_{13} & c_{33} & 0 & 0 & 0 \\ 0 & 0 & 0 & c_{44} & 0 & 0 \\ 0 & 0 & 0 & 0 & c_{44} & 0 \\ 0 & 0 & 0 & 0 & 0 & \frac{c_{11}-c_{12}}{2} \end{bmatrix} \begin{bmatrix} \epsilon_1 \\ \epsilon_2 \\ \epsilon_3 \\ \epsilon_4 \\ \epsilon_5 \\ \epsilon_6 \end{bmatrix}, \quad (1)$$

where  $\sigma_i$  and  $\epsilon_i$  ( $i=1, \dots, 6$ ) represent the stresses and strains, respectively. There are only five independent elastic constants:  $c_{11}$ ,  $c_{12}$ ,  $c_{13}$ ,  $c_{33}$ , and  $c_{44}$ . Their values in the present work are listed in Table II.

Similarly, the piezoelectricity can be expressed in the matrix form:<sup>37</sup>

$$\begin{bmatrix} P_1 \\ P_2 \\ P_3 - P_3^0 \end{bmatrix} = \begin{bmatrix} 0 & 0 & 0 & 0 & e_{15} & 0 \\ 0 & 0 & 0 & e_{15} & 0 & 0 \\ e_{31} & e_{31} & c_{33} & 0 & 0 & 0 \end{bmatrix} \begin{bmatrix} \epsilon_1 \\ \epsilon_2 \\ \epsilon_3 \\ \epsilon_4 \\ \epsilon_5 \\ \epsilon_6 \end{bmatrix}, \quad (2)$$

where  $P_1$ ,  $P_2$ , and  $P_3$  are three polarization components along **a** direction, the direction perpendicular to **a** and **c**, and **c** direction, respectively.  $P_3^0$  is the spontaneous polarization along **c** direction. There are only 3 independent piezoelectric coefficients:  $e_{31}$ ,  $e_{33}$ , and  $e_{15}$ . It is necessary to point out that here the definition of piezoelectricity is different from that in Ref. 37 where the piezoelectricity reflects the relation between polarizations and stresses. The piezoelectric coefficients obtained by the present work are listed in Table III.

Good agreements have been achieved between the present results and those in literatures (see Tables II and III). Confirming that our computational procedure can give reasonable results for bulk ZnO systems, we proceed to analyze ZnO single layers and nanotubes.

### III. ZINC OXIDE SINGLE LAYERS

In this section, we discuss the elasticity and piezoelectricity of ZnO single layers. First, as an initial configuration, we take a single Zn-O layer (shown in the left side of Fig. 1) cut

from the wurtzite ZnO crystal, and then optimize its structure. As an stable configuration, we obtain a planar graphite-like structure as shown in the right side of Fig. 1. Here we use  $6 \times 6 \times 1$  Monkhorst-Pack k-points and two different groups of other input parameters for calculations. The final optimized results, listed in Table IV, are insensitive to the input parameters. The bond length of the planar structure is slightly smaller than that of ZnO crystals. Its binding energy is  $-8.246$  eV/ZnO, higher than the value  $-8.947$  eV/ZnO of ZnO crystals.

Now we consider a wurtzite ZnO thin film with two polar surfaces ( $\pm 0001$  faces). Its energy is higher than that of bulk ZnO with the same number of atoms by  $E_c = 4.0$  J/m<sup>2</sup> (the cleavage energy density<sup>40</sup>) because of the spontaneous polarization in  $c$  direction. Here we derive the critical layer number based on our above result for planar ZnO single layers. Considering the influence of spontaneous polarization, we estimate the total binding energy  $E_f = M(-8.947N + E_c\Omega_0) = M(-8.947N + 2.21)$  eV for the wurtzite thin film with  $N$  Zn-O single layers, where  $\Omega_0$  is the area for a unit cell of the ZnO crystal in  $ab$  plane and  $M$  the number of unit cells in each layer. If we consider the thin film with  $N$  planar single layers and neglect the very weak interlayer attractions, the total binding energy is about  $-8.246MN$  eV. We find  $E_f > -8.246MN$  for  $N < 4$ , which implies that a ZnO thin film less than  $N_c = 4$  Zn-O layers prefers the planar graphite-like structure to the wurtzite structure. Here the estimated value 4 is the lower bound of critical number  $N_c$  because we neglect the weak interlayer attractions. Note that the cleavage energy density may depend on the layer number and structural relaxation. Considering the structural relaxation, Meyer and Marx<sup>41</sup> found that the cleavage energy density varied from  $3.0$  J/m<sup>2</sup> to  $3.4$  J/m<sup>2</sup>, weakly dependent on the layer number. Using these values, the lower bound of critical number  $N_c$  is changed to 3. If we consider the interlayer attractions coming from the dipole-dipole interaction between planar ZnO layers because of their spontaneous polarizations (the ground state: spontaneous polarizations antiparallel in the neighbor layers), we should obtain  $N_c > 3$ , which is the exact meaning of “the lower bound of critical number being 3”. Claeysens *et al.* also obtained a critical thickness by DFT calculations.<sup>42</sup> They investigated the binding energy of the thin films with  $N = 4, 6, \dots, 24$  single planar layers (layer distance  $2.4$  Å) and compared it with the binding energy of the thin films (wurtzite structure) with the same number of Zn-O layers. They found that the ZnO thin film less than eighteen Zn-O layers prefers the planar graphite-like structure to the wurtzite structure. As is well known,

the widely used DFT packages cannot accurately describe the interlayer interactions.<sup>43,44</sup> Thus the critical layer number  $N_c = 18$  obtained directly from DFT calculations might be inaccurate although it satisfies  $N_c > 3$ . With the development of DFT method, one may obtain the accurate critical layer number in the future when DFT packages can deal well with the interlayer interactions.

Adopting the optimized structure, we can calculate the elastic and piezoelectric constants of ZnO single layers. From Fig. 2, we find that the ZnO single layer has the 3-fold rotation symmetry and a reflection symmetry respect to  $x_1$ -axis. Thus the stress-strain relation is expressed in the matrix form:<sup>37</sup>

$$\begin{bmatrix} \sigma_1 \\ \sigma_2 \\ \sigma_6 \end{bmatrix} = \begin{bmatrix} c_{11} & c_{12} & 0 \\ c_{12} & c_{11} & 0 \\ 0 & 0 & \frac{c_{11}-c_{12}}{2} \end{bmatrix} \begin{bmatrix} \epsilon_1 \\ \epsilon_2 \\ \epsilon_6 \end{bmatrix}. \quad (3)$$

There are only two independent elastic constants:  $c_{11}$  and  $c_{12}$ . The piezoelectricity can be expressed as

$$\begin{bmatrix} P_1 - P_1^0 \\ P_2 \end{bmatrix} = \begin{bmatrix} e_{11} & -e_{11} & 0 \\ 0 & 0 & -e_{11} \end{bmatrix} \begin{bmatrix} \epsilon_1 \\ \epsilon_2 \\ \epsilon_6 \end{bmatrix}, \quad (4)$$

where  $P_1^0$  is the spontaneous polarization in the  $x_1$ -direction. There is only one independent piezoelectric coefficient  $e_{11}$ . The calculated values of the elastic and piezoelectric constants of ZnO single layers are listed in Table V. Using the elastic constants, we calculate the Young's modulus per atom by  $Y_{atom} = (c_{11} - c_{12}^2/c_{11})/2 \approx 32.4$  eV/atom, which is quite smaller than the value 57.7 eV/atom for a single graphite layer obtained in our previous work.<sup>45</sup> Additionally, we observe that the ZnO single layer ( $e_{11} = 0.48$  e/Å) has stronger piezoelectricity than the BN single layer ( $e_{11} = 0.23$  e/Å).<sup>46</sup>

#### IV. SINGLE-WALLED ZINC OXIDE NANOTUBES

Generally speaking, if a material can exist in graphite-like structure, the corresponding nanotubes can be synthesized in the laboratory.<sup>13</sup> A natural question is: how can we fabricate SWZONTs? We propose a possible way in this section.

Without considering the two ends, an SWZONT can be thought of as a cylinder rolled up from a single sheet of ZnO layer such that two equivalent sites of the hexagonal lattice

coincide. To describe the SWZONT, we introduce several characteristic vectors in analogy with a single-walled carbon nanotube. As shown in Fig. 2, the chiral vector  $\mathbf{C}_h$ , which defines the relative location of two sites, is specified by a pair of integers  $(n, m)$  which is called the index of the SWZONT and relates  $\mathbf{C}_h$  to two unit vectors  $\mathbf{a}_1$  and  $\mathbf{a}_2$  of the hexagonal lattice ( $\mathbf{C}_h = n\mathbf{a}_1 + m\mathbf{a}_2$ ). The chiral angle  $\theta$  defines the angle between  $\mathbf{a}_1$  and  $\mathbf{C}_h$ . For an  $(n, m)$  nanotube,  $\theta = \arccos[(2n+m)/(2\sqrt{n^2+m^2+nm})]$ . The translational vector  $\mathbf{T}$  corresponds to the first point in the hexagonal lattice through which the line normal to the chiral vector  $\mathbf{C}_h$  passes.

We calculate the binding energy of SWZONTs with different indexes which is shown in Fig. 3. From this figure we find that: (i) The binding energy for different SWZONTs is negative, which suggests these SWZONTs can exist in principle; (ii) The binding energy ( $E_b$ ) decreases with the increase of the radius ( $R$ ) of SWZONTs and can be well fit by

$$E_b = -8.242 + 1.371/R^2 \quad (\text{eV/ZnO}). \quad (5)$$

Obviously,  $E_b \rightarrow -8.242 \text{ eV/ZnO}$  for  $R \rightarrow \infty$ . This value is quite close to the binding energy ( $-8.246 \text{ eV/ZnO}$ ) of a ZnO single planar layer. The term  $1.371/R^2$  reflects the curvature effect of nanotubes. The classic shell theory also gives the same form,  $D\Omega/R^2$ , for the curvature effect,<sup>47</sup> where  $D$  is the rigidity of the ZnO single layer and  $\Omega = 8.91 \text{ \AA}^2$  is the area of the parallelogram generated by the unit vectors  $\mathbf{a}_1$  and  $\mathbf{a}_2$ . Thus we obtain  $D = 0.15 \text{ eV}$ , which is quite smaller than the rigidity ( $1.17 \text{ eV}$ )<sup>48</sup> of a single graphite layer. The ZnO single layer is much softer than the graphite layer such that it should be more easily wrapped up into a nanotube.

The solid-vapor phase process has been employed to successfully synthesize ZnO nanobelts, nanorings, and nanohelices.<sup>7,8,9,10</sup> It might also be used to realize SWZONTs with carbon nanotubes as templates. As shown in Fig. 4, the ZnO powder decomposes into gaseous  $\text{Zn}^{2+}$  and  $\text{O}^{2-}$  at high temperature and low pressure.<sup>49</sup> After that, Ar flow carries  $\text{Zn}^{2+}$  and  $\text{O}^{2-}$  to the low temperature zone at relative higher pressure where  $\text{Zn}^{2+}$  and  $\text{O}^{2-}$  will deposit on the carbon nanotube array prepared carefully in advance. Controlling the low enough density of  $\text{Zn}^{2+}$  and  $\text{O}^{2-}$  and the proper distance between carbon nanotubes, one may obtain thin enough ZnO films, for example less than 3 single layers, coating on the surfaces of carbon nanotubes. These films prefer the multi-walled tubes to the wurtzite structure because the layer number is smaller than 3. One may take out the SWZONTs

from the multi-walled tubes by analogy with the method in carbon nanotubes.<sup>50</sup>

Now we discuss two points in the above process. The first point is the growth temperature. From the conditions for producing ZnO nanobelts,<sup>7,8,9,10</sup> the growth temperature of ZnO nanotubes is expected to be 300–500 °C. At this temperature, the highly purified carbon nanotubes are chemically inactive,<sup>51</sup> which ensures that they merely work as templates but do not react with  $\text{Zn}^{2+}$  or  $\text{O}^{2-}$ . The other point is the critical radius of the synthesized SWZONTs. The carbon-ZnO multi-walled tubes can form in the above process if the attraction between nanotubes overcomes the curvature energy of ZnO nanotubes. For simplicity, we consider a carbon nanotube coated by an SWZONT. The attraction between them is approximately described by the Lennard-Jones potential. The layer distance is estimated to be 3–4 Å from the van der waals radii of carbon, oxygen, and zinc atoms.<sup>52</sup> The attraction energy ( $E_{at}$ ) is about  $-19.5 \text{ meV/ZnO}$ .<sup>53</sup> From  $E_{at} + D\Omega/R^2 < 0$ , we obtain the smallest radius  $R_c \sim 8.3 \text{ Å}$  synthesized in the above process. We should emphasize that the above process is merely possible method to produce the ZnO nanotubes in terms of the first-principles calculation and the previous experiments<sup>7,8,9,10</sup> on the growth of ZnO nanobelts. Whether it works or not, experimental researches will give an answer in the future.

It is useful to discuss the piezoelectricity of SWZONTs. We need not to do additional DFT calculations considering the experience obtained by Sai *et al.* in the study of the piezoelectricity of single-walled BN nanotubes.<sup>46</sup> They found that the piezoelectricity of BN nanotubes depends on the chirality. The physical origin is that an angle between local polarization of each unit cell and the tube axis depends on the chiral angle. Their key point is that the curvature of nanotubes has so small effect on the piezoelectricity that we can directly deduce their piezoelectric property from the piezoelectricity of single layers. Two deformation modes will result in the change of the polarization in the direction of tube axis: one is the tension or compression strain ( $\varepsilon_T$ ) along the tube axis, another is the shear strain ( $\gamma$ , the twist angle per length) induced by the torsion around the tube axis. The variation of the polarization can be expressed as

$$\delta P_T/L = e_T \varepsilon_T + e_t \gamma, \quad (6)$$

where  $L$  represents the perimeter of the nanotube. Following Ref.46, one can derive the



coefficients

$$e_T = e_{11} \cos 3\theta \quad (7)$$

and

$$e_t = -e_{11} \sin 3\theta \quad (8)$$

from the transformation between coordinate systems  $\{x_1, x_2\}$  and  $\{\mathbf{C}_h, \mathbf{T}\}$  shown in Fig. 2. From above three equations, we find that the piezoelectricity of SWZONTs depends on their chiral angles. For zigzag tubes ( $m = 0, \theta = 0^\circ$ ), only tension or compression strains induce polarizations, while only shear strains play roles for armchair tubes ( $n = m, \theta = 30^\circ$ ). Both strains work for achiral tubes. For a specific pure axial strain, the variation of the polarization decreases with the increase of chiral angle  $\theta$  from  $0^\circ$  to  $30^\circ$ . For pure shear strain induced by the torsion around the tube axis, the absolute variation of the polarization increases with the increase of chiral angle  $\theta$  from  $0^\circ$  to  $30^\circ$ . These effects are more evident in SWZONTs than in BN nanotubes because the ZnO single layer has a relative larger  $e_{11}$  than the BN single layer.

## V. CONCLUSION

We have calculated the elastic constants and piezoelectric coefficients of ZnO crystals and single layers. We find that ZnO single layers are much more flexible than graphite single layers in the elasticity and stronger than boron nitride single layers in the piezoelectricity. SWZONTs are demonstrated to exist in principle and might be realized by the solid-vapor phase process with carbon nanotubes as templates.

Finally, we would like to point out some potential applications of SWZONTs and related structures. (i) SWZONTs, same as other ZnO nanostructures, can be applied in optoelectric devices. The quality of SWZONT-based devices should be higher than others because of their very small thickness. (ii) The piezoelectricity of SWZONTs depends on their chirality. For most ZnO nanotubes except the zigzag type, twists around the tube axis will induce axial polarizations. This property makes SWZONTs possible to be used in the torsion measurement devices. For example, one may use SWZONTs to make very small Coulomb torsion balance. (iii) SWZONTs, except the armchair tubes, are polar tubes.<sup>54</sup> Water transport, ice formation, and biopolymer translocation in polar tubes should exhibit quite different characteristics from those in non-polar tubes. The latter has been fully studied, especially

for carbon nanotubes,<sup>55,56,57</sup> while the former has attracted no attention even for BN tubes up to now. (iv) The carbon-ZnO nanotubes formed in the solid-vapor phase process must have excellent mechanical and electrical properties: On the one hand, they have high enough rigidity and axial strength because of the contribution of carbon nanotubes. On the other hand, they exhibit strong piezoelectricity coming from the ZnO tubes. These structures may be employed to make electric nanotube motors<sup>58</sup> where the axial voltage will be greatly reduced relative to carbon nanotube motors<sup>58</sup> because of the high piezoelectricity of ZnO tubes.

### Acknowledgements

We are very grateful to the kind help of Dr. Q. X. Li and Y. D. Liu. Calculations have been performed on Numerical Materials Simulator (HITACHI SR11000) at the Computational Materials Science Center, National Institute for Materials Science.

- 
- <sup>1</sup> Ü. Özgür, Y. I. Alivov, C. Liu, A. Teke, M. A. Reshchikov, S. Doğan, V. Avrutin, S. J. Cho, and H. Morkoç, *J. Appl. Phys.* **98**, 041301 (2005).
  - <sup>2</sup> Z. L. Wang, *Mater. Today* **7**, 26 (2004).
  - <sup>3</sup> Z. L. Wang, *J. Phys.: Condens. Matter* **16**, R829 (2004).
  - <sup>4</sup> M. H. Huang, S. Mao, H. Feick, H. Yan, Y. Wu, H. Kind, E. Weber, R. Russo, P. Yang, *Science* **292**, 1897(2001).
  - <sup>5</sup> M. Haupt, A. Ladenburger, R. Sauer, K. Thonke, R. Glass, W. Roos, J. P. Spatz, H. Rauscher, S. Riethmüller, and M. Möller, *J. Appl. Phys.* **93**, 6252 (2003).
  - <sup>6</sup> W. I. Park, D. H. Kim, S. W. Jung, and G. C. Yi, *Appl. Phys. Lett.* **80**, 4232 (2002).
  - <sup>7</sup> Z. W. Pan, Z. R. Dai, and Z. L. Wang, *Science* **291**, 1947 (2001).
  - <sup>8</sup> X. Y. Kong and Z. L. Wang, *Nano Lett.* **3**, 1625 (2003).
  - <sup>9</sup> W. L. Hughes and Z. L. Wang, *J. Am. Chem. Soc.* **126**, 6703 (2004).
  - <sup>10</sup> X. Y. Kong, Y. Ding, R. Yang, and Z. L. Wang, *Science* **303**, 1348 (2004).
  - <sup>11</sup> M. S. Arnold, P. Avouris, Z. W. Pan, and Z. L. Wang, *J. Phys. Chem. B* **107**, 659 (2003).
  - <sup>12</sup> S. Iijima, *Nature (London)* **354**, 56 (1991).

- <sup>13</sup> C. N. R. Rao and M. Nath, Dalton Trans. **2003**, 1 (2003).
- <sup>14</sup> J. Q. Hu, Q. Li, X. M. Meng, C. S. Lee, and S. T. Lee, Chem. Mater. **15**, 305 (2003).
- <sup>15</sup> Y. J. Xing, Z. H. Xi, Z. Q. Xue, X. D. Zhang, J. H. Song, R. M. Wang, J. Xu, Y. Song, S. L. Zhang, and D. P. Yu, Appl. Phys. Lett. **83**, 1689 (2003).
- <sup>16</sup> Y. J. Xing, Z. H. Xi, X. D. Zhang, J. H. Song, R. M. Wang, J. Xu, Z. Q. Xue and D. P. Yu, Solid State Commun. **129**, 671 (2004).
- <sup>17</sup> R. M. Wang, Y. J. Xing, J. Xu and D. P. Yu, New J. Phys. **5**, 115 (2003).
- <sup>18</sup> Y. Sun, G. M. Fuge, N. A. Fox, D. J. Riley, and M. N. R. Ashfold, Adv. Mat. **17**, 2477 (2005).
- <sup>19</sup> X. Y. Kong, Y. Ding, Z. L. Wang, J. Phys. Chem. B. **108**, 570 (2004).
- <sup>20</sup> G. S. Wu, T. Xie, X. Y. Yuan, Y. Li, L. Yang, Y. H. Xiao, and L. D. Zhang, Solid State Commun. **134**, 485 (2005).
- <sup>21</sup> J. F. Yan, Y. M. Lu, H. W. Liang, Y. C. Liu, B. H. Li, X. W. Fan, and J. M. Zhou, J. Crystal Growth **280**, 206 (2005).
- <sup>22</sup> X. H. Zhang, S. Y. Xie, Z. Y. Jiang, X. Zhang, Z. Q. Tian, Z. X. Xie, R. B. Huang, and L. S. Zheng, J. Phys. Chem. B. **107**, 10114 (2003).
- <sup>23</sup> J. J. Wu, S. C. Liu, C. T. Wu, K. H. Chen, and L. C. Chen, Appl. Phys. Lett. **81**, 1312 (2002).
- <sup>24</sup> J. Zhang, L. Sun, C. Liao, and C. Yan, Chem. Commun. 2002, 262 (2002).
- <sup>25</sup> X. Gonze, J. M. Beuken, R. Caracas, F. Detraux, M. Fuchs, G. M. Rignanese, L. Sindic, M. Verstraete, G. Zerah, F. Jollet, M. Torrent, A. Roy, M. Mikami, Ph. Ghosez, J. Y. Raty, and D. C. Allan, Comput. Mater. Sci. **25**, 478 (2002).
- <sup>26</sup> P. Hohenberg and W. Kohn, Phys. Rev. **136**, B864 (1964); W. Kohn and L. J. Sham, *ibid.* **140**, A1133 (1965).
- <sup>27</sup> X. Gonze, Phys. Rev. A **52**, 1086 (1995); **52**, 1096 (1995); X. Gonze, Phys. Rev. B **55**, 10337 (1997); X. Gonze and C. Lee, *ibid.* **55**, 10355 (1997).
- <sup>28</sup> S. Baroni, S. de Gironcoli, A. D. Corso, and P. Giannozzi, Rev. Mod. Phys. **73**, 515 (2001).
- <sup>29</sup> D. R. Hamann, X. Wu, K. Rabe, and D. Vanderbilt, Phys. Rev. B **71**, 035117 (2005).
- <sup>30</sup> H. Karzel, W. Potzel, M. Köfferlein, W. Schiessl, M. Steiner, U. Hiller, G. M. Kalvius, D. W. Mitchell, T. P. Das, P. Blaha, K. Schwarz, and M. P. Pasternak, Phys. Rev. B **53**, 11425 (1996).
- <sup>31</sup> N. Troullier and J. L. Martins, Phys. Rev. B **43**, 1993(1991).
- <sup>32</sup> H. J. Monkhorst and J. D. Pack, Phys. Rev. B **13**, 5188 (1976).
- <sup>33</sup> D. M. Ceperley and B. J. Alder, Phys. Rev. Lett. **45**, 566 (1980).

- <sup>34</sup> J. P. Perdew and Y. Wang, Phys. Rev. B **45**, 13244 (1992).
- <sup>35</sup> X. Wu, D. Vanderbilt, and D. R. Hamann, Phys. Rev. B **72**, 035105 (2005).
- <sup>36</sup> M. Catti, Y. Noel, and R. Dovesi, J. Phys. Chem. Solids **64**, 2183 (2003).
- <sup>37</sup> J. F. Nye, *Physical Properties of Crystals* (Clarendon Press, Oxford, 1985).
- <sup>38</sup> I. B. Kobiakov, Solid State Commun. **35**, 305 (1980).
- <sup>39</sup> T. Azuhata, M. Takesada, T. Yagi, A. Shikanai, S. F. Chichibu, K. Torii, A. Nakamura, T. Sota, G. Cantwell and D. B. Eason, C. W. Litton, J. Appl. Phys. **94**, 968 (2003).
- <sup>40</sup> A. Wander, F. Schedin, P. Steadman, A. Norris, R. McGrath, T. S. Turner, G. Thornton, and N. M. Harrison, Phys. Rev. Lett. **86**, 3811 (2001).
- <sup>41</sup> B. Meyer and D. Marx, Phys. Rev. B **67**, 035403 (2003).
- <sup>42</sup> F. Claeysens, C. L. Freeman, N. L. Allan, Y. Sun, M. N. R. Ashfold, and J. H. Harding, J. Mater. Chem. **15**, 139 (2005).
- <sup>43</sup> Y. Andersson, D. C. Langreth, and B. I. Lundqvist, Phys. Rev. Lett. **76**, 102 (1996).
- <sup>44</sup> W. Kohn, Y. Meir, and D. E. Makarov, Phys. Rev. Lett. **80**, 4153 (1998).
- <sup>45</sup> Z. C. Tu and Z. C. Ou-Yang, Phys. Rev. B **65**, 233407 (2002).
- <sup>46</sup> N. Sai and E. J. Mele, Phys. Rev. B **68**, 241405(R) (2003).
- <sup>47</sup> L. D. Landau and E. M. Lifshiz, *Theory of Elasticity* (Pergamon, Oxford, 1986).
- <sup>48</sup> O. Y. Zhong-can, Z. B. Su, and C. L. Wang, Phys. Rev. Lett. **78**, 4055 (1997).
- <sup>49</sup> D. Kohl, M. Henzler, and G. Heiland, Surf. Sci. **41**, 403 (1974).
- <sup>50</sup> J. Cumings and A. Zettl, Science **289**, 602 (2000).
- <sup>51</sup> P. M. Ajayan, T. W. Ebbesen, T. Ichihashi, S. Iijima, K. Tanigaki, and H. Hiura, Nature **362**, 522 (1993).
- <sup>52</sup> H. Partridge, J. R. Stallcop, and E. Levin, J. Chem. Phys. **115**, 6471 (2001).
- <sup>53</sup> The characteristic energy of van der Waals interactions (in Lennard-Jones form) between carbon atoms, oxygen atoms, and zinc atoms is taken from Ref. 52:  $\varepsilon_C = -24.95$  K,  $\varepsilon_O = -22.75$  K,  $\varepsilon_{Zn} = -111.37$  K. Using the combination law of Lennard-Jones potentials, we obtain the characteristic energy of interactions between carbon and oxygen atoms, and carbon and zinc atoms as  $\varepsilon_{C-O} = -(\varepsilon_C \varepsilon_O)^{1/2} = -2.0$  meV,  $\varepsilon_{C-Zn} = -(\varepsilon_C \varepsilon_{Zn})^{1/2} = -4.5$  meV. Roughly speaking, each zinc and oxygen atoms interact with three nearest neighbor carbon atoms. The attraction energy ( $E_{at}$  per ZnO) between ZnO tube and carbon tube is estimated as  $E_{at} = -3(\varepsilon_{C-Zn} + \varepsilon_{C-O})$ .

- <sup>54</sup> Ş. Erkoç and H. Kökten, Physica E **28**, 162 (2005).
- <sup>55</sup> G. Hummer, J. C. Rasaiah, and J. P. Noworyta, Nature **414**, 188 (2001).
- <sup>56</sup> K. Koga, G. T. Gao, H. Tanaka, and X. C. Zeng, Nature **412**, 802 (2001).
- <sup>57</sup> H. Gao, Y. Kong, D. Cui, and C. S. Ozkan, Nano Lett. **4**, 471 (2003).
- <sup>58</sup> Z. C. Tu and X. Hu, Phys. Rev. B **72**, 033404 (2005).

TABLE I: Structure parameters of ZnO crystals.

Authors	Methods	$a$ (Å)	$c$ (Å)	$c/a$	u
Present	DFT	3.199	5.167	1.615	0.379
Karzel <i>et al.</i> <sup>a</sup>	Experiment	3.250	5.204	1.602	0.382
Wu <i>et al.</i> <sup>b</sup>	DFT	3.197	5.166	1.616	0.380
Catti <i>et al.</i> <sup>c</sup>	Hartree-Fock	3.286	5.241	1.595	0.383

<sup>a</sup>Reference 30.

<sup>b</sup>Reference 35.

<sup>c</sup>Reference 36.

TABLE II: Elastic constants (relaxed-ions) of ZnO crystals in units of GPa.

Authors	Methods	$c_{11}$	$c_{12}$	$c_{13}$	$c_{33}$	$c_{44}$
Present	DFPT	218	137	121	229	38
Wu <i>et al.</i> <sup>a</sup>	DFPT	226	139	123	242	40
Catti <i>et al.</i> <sup>b</sup>	Hartree-Fock	246	127	105	246	56
Kobiakov <sup>c</sup>	Experiment	207	118	106	210	45
Azuhata <i>et al.</i> <sup>d</sup>	Experiment	190	110	90	196	39

<sup>a</sup>Reference 35.

<sup>b</sup>Reference 36.

<sup>c</sup>Reference 38.

<sup>d</sup>Reference 39.

TABLE III: Piezoelectric coefficients (relaxed-ions) of ZnO crystals in units of C/m<sup>2</sup>.

Authors	Methods	$e_{31}$	$e_{33}$	$e_{15}$
Present	DFPT	-0.65	1.24	-0.54
Wu <i>et al.</i> <sup>a</sup>	DFPT	-0.67	1.28	-0.53
Catti <i>et al.</i> <sup>b</sup>	Hartree-Fock	-0.55	1.19	-0.46
Kobiakov <sup>c</sup>	Experiment	-0.62	0.96	-0.37

<sup>a</sup>Reference 35.

<sup>b</sup>Reference 36.

<sup>c</sup>Reference 38.

TABLE IV: Optimized structure of a ZnO single layer. Here  $L_v$ ,  $B_l$ ,  $B_a$ , and  $E_b$  represent the vacuum layer thickness, bond length, bond angle, and binding energy, respectively.

$L_v$ (Å)	ecut (Ha)	$B_l$ (Å)	$B_a$	$E_b$ (eV/ZnO)
10.6	35	1.852	120°	-8.246
21.2	60	1.852	120°	-8.247

TABLE V: Elastic and piezoelectric constants (relaxed-ions) of ZnO single layers. Here  $L_v$  represents the vacuum layer thickness.

$L_v$ (Å)	ecut (Ha)	$c_{11}$ (eV/ZnO)	$c_{12}$ (eV/ZnO)	$e_{11}$ (e/Å)
10.6	35	72.6	24.0	0.48
21.2	60	72.7	24.1	0.48

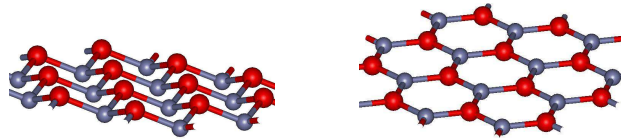


FIG. 1: (Color online) ZnO single layers. The left side is a single layer taken from the wurtzite ZnO crystal while the right one is the optimized structure which is a planar hexagonal lattice. The small and large balls represent zinc and oxygen atoms, respectively.

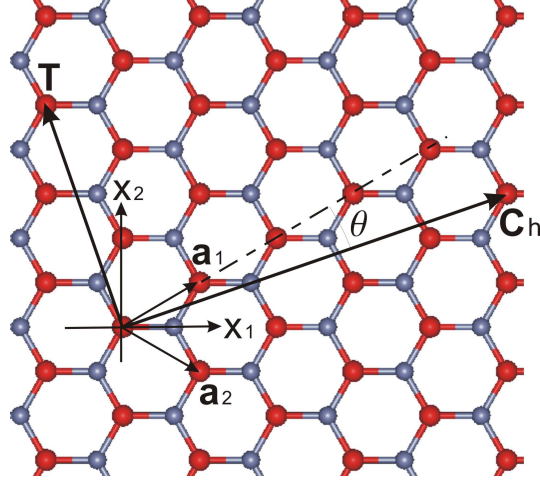


FIG. 2: (Color online) Unrolled honeycomb lattice of an SWZONT. By rolling up the sheet such that the atoms in the two ends of the vector  $\mathbf{C}_h$  coincide, a nanotube is formed. The vectors  $\mathbf{a}_1$  and  $\mathbf{a}_2$  are unit vectors of the hexagonal lattice. The translational vector  $\mathbf{T}$  is perpendicular to  $\mathbf{C}_h$  and runs in the direction of the tube axis.

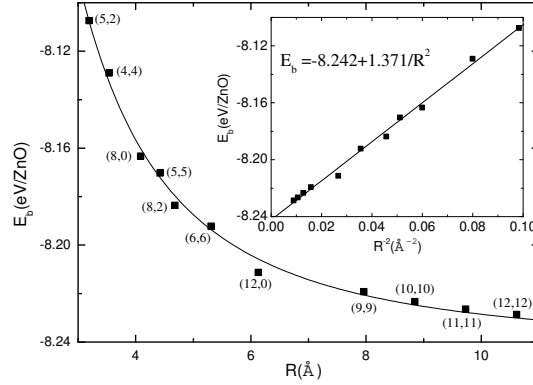


FIG. 3: Binding energy ( $E_b$ ) and radius ( $R$ ) of different SWZONTs.

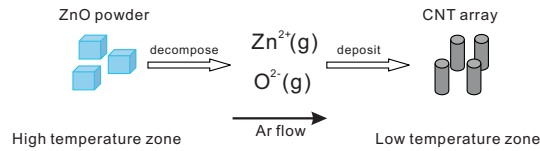


FIG. 4: (Color online) Schematic diagram of the vapor-solid phase process to synthesize SWZONTs with carbon nanotube (CNT) array as templates.